Gravitational Search Algorithm-based Photovoltaic Array Reconfiguration for Partial Shading Losses Reduction

Hany M. Hasanien, Ahmed Al-Durra†, and S. M. Muyeen†*

**Electrical Power and Machines Department, Faculty of Engineering, Ain Shams University, Cairo 11517, Egypt (hanyhasanien@ieee.org), †Department of Electrical Engineering, The Petroleum Institute, Abu Dhabi 2533, UAE*

Keywords: Array reconfiguration, gravitational search algorithm, partial shading, photovoltaic (PV) module, PV systems.

Abstract

The operation of a photovoltaic (PV) array under partial shading (PS) conditions represents a great challenge in the PV systems. The PS of a PV array causes a reduction of the generated power of such array and increases the thermal losses inside the shaded modules. This paper presents the gravitational search algorithm (GSA) to optimally fully reconfigure the PV array with the purpose of reducing the PS losses. The single diode PV model is used to model the PV module. The GSA code is built using MATLAB environment. The target of the optimized problem is to minimize the irradiance level mismatch index. The reconfigurable PV array is modelled using MATLAB/SIMULINK environment. The validity of the GSA-based reconfigurable PV array is verified by the simulation results. The effectiveness of proposed PV array is evaluated by comparing its results with that of other PV array configurations under different PS and PV modules conditions.

1 Introduction

The photovoltaic (PV) system will be one of the most promising renewable energy systems in the near future. The costs of installed PV systems are continuously decreasing worldwide because of dropping component average selling prices [1]. The global PV system installations reached 136.7 GW at the end of 2013 and the cumulative market growth reached 36% [2]. The large scale PV power plants were connected to the grid in the last few years. One of the problems facing the PV system is its operation under partial shading (PS) conditions.

There are many factors causing the PS of a PV array. Neighboring buildings, trees, and even other PV arrays can cause the PS of PV array. In these cases, PS can be easily avoided by the proper design of the PV system. Other factors are difficult to be avoided such as clouds, dust, and snow. The PS of the PV arrays causes annual energy losses [3].

The PV modules of partially shaded PV array receive non-uniform solar irradiations resulting in multiple peaks of the power versus voltage (*P-V*) characteristics. Therefore, the global peak or maximum power point (MPP) may be misleading and this causes a reduction of the generated power of the PV array [4]-[8]. The PS can cause the shaded modules to act as loads consuming power and increasing the thermal losses. This is because of the operation of shaded modules in the reverse bias region [9]. Another type of the PS losses is the application of the bypass diodes which are utilized to avoid hot spots formed in the partially shaded PV array. Turning the diodes on creates losses due to their forward-biased resistances [10].

To mitigate the PS effects and extracting the maximum power of a partially shaded PV array, several techniques have been used. Some methods rely on modifications of the maximum power point tracking (MPPT) techniques that detect the global peak [9]. Another category includes different PV architecture such as micro-inverters. Some approaches depend on the converter topology such as the multilevel converter. However, these methods suffer from the complex control. Other methods contain different array configuration for interconnecting PV modules such as series-parallel, total-cross-tied (TCT), and bridge-linked configurations [10].

The PV array reconfiguration is an active technique used to reconfigure PV modules of the PS PV array using solid state switches. The main target of reconfiguration is the reduction of PS losses. In [11], an adaptive reconfiguration of the PS PV array is presented to reduce the PS effects. The PV array is divided into fixed and adaptive parts with a switching matrix. Simple control schemes are used to optimize the output power. However, the modifications of the proposed algorithms to deal with a large number of reconfigurable columns are not mentioned. In [12], a dynamic PV array reconfiguration is introduced for a grid-connected PV system. The proposed optimal reconfiguration is based on minimization of the irradiance equalization index, which is the difference between the maximum and minimum average row irradiance levels in the PV array. However, the differences in the rows irradiance levels should be minimized to yield an optimal reconfiguration. In [10], an optimal reconfiguration of a PV array is proposed. The optimized problem is considered as a mixed integer quadratic programming (MIQP) problem and its optimal solution is determined using a branch and bound algorithm. Although, the maximum allowable output power of the partially shaded PV array is reached using this algorithm, the time required to perform the optimization process is longer resulting in inefficient usage in real time applications. The great development of the meta-heuristic optimization techniques represents the impetus for using the gravitational search algorithm (GSA) to optimally reconfigure the PS PV array for the PS loss reduction.

The GSA is a meta-heuristic physics-based optimization technique presented by Rashedi *et al.* in 2009 [13]. The principle of GSA depends on Newton gravitational law and the law of motion. The GSA has been successfully applied to solve many power system optimization problems such as optimal reactive power dispatch [14], [15], optimal power flow [16], and multi-distributed generation planning [17]. Recently, it has been explored in electric machines design such as magnetizers design [18].

In this paper, the GSA is presented to optimally fully reconfigure the PV array with the purpose of reducing the PS losses. The single diode PV model is used to model the PV module. The target of the optimized problem is to minimize the irradiance level mismatch index. The reconfigurable PV array is modeled using MATLAB/SIMULINK environment. The validity of the GSA-based reconfigurable PV array is verified by the simulation results. The effectiveness of proposed PV array is evaluated by comparing its results with the results of other PV array configurations under different PS conditions and PV modules.

2 Model of PV Module

The single diode model of the PV module is illustrated in Fig. 1. The *I-V* characteristic of PV module can be written as follows [19]:

$$I = I_{PV} - I_o \left[\exp\left(\frac{V+R_s I}{a\,V_t}\right) - 1\right] - \frac{V+R_s I}{R_p} \quad (1)$$

where I_{PV} is the photovoltaic current, I_o is the reverse saturation current of the diode, a is the ideality factor of the diode, and V_t is the thermal voltage of the module. R_s and R_p are the series and parallel resistance, respectively. I_{PV} is written by the following formula:

$$I_{PV} = \left(I_{PV,n} + K_I\,\Delta T\right)\frac{G}{G_n} \quad (2)$$

where $I_{PV,n}$ is the photovoltaic current under the nominal condition. K_I is the short circuit current per temperature coefficient, ΔT is the difference between the actual and nominal temperatures, G and G_n are the actual and normal solar irradiation [20]. $I_{PV,n}$ is given by

$$I_{PV,n} = \frac{R_p+R_s}{R_p}\,I_{sc,n} \quad (3)$$

The reverse saturation current I_o is deeply influenced by the temperature and it can be mathematically modeled by the following equation [20]:

$$I_o = \frac{I_{sc,n}+K_I\Delta T}{exp\left(\frac{(V_{oc,n}+K_V\Delta T)}{a\,V_t}\right)-1} \quad (4)$$

where $I_{sc,n}$, and $V_{oc,n}$ are the short circuit current and open circuit voltage under the nominal condition, respectively. K_V is the open circuit voltage per temperature coefficient.

3 Problem Formulation

The PS phenomena of the PV array results in an irradiance level mismatch between the PV modules. The implementation

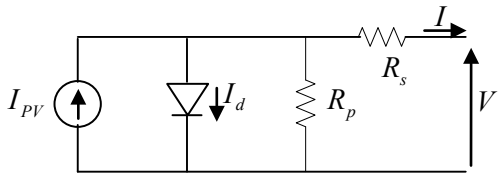

Fig. 1. Equivalent circuit of the single diode PV model.

of dynamic PV array reconfiguration plays an important role in minimizing irradiance level mismatch on the row level. The irradiance level mismatch index (*IMI*) can be defined as the sum of squares of the differences between the total irradiance levels of the PV rows. It can be mathematically modeled by the following equation [10]:

$$IMI = \sum_{i=1}^{m}\sum_{l=1}^{m}\left(\frac{G_{ti}}{G_n} - \frac{G_{tl}}{G_n}\right)^2 \quad (5)$$

where G_{ti} and G_{tl} are the total irradiance levels of the rows i and l, respectively. m is the number of PV rows.

The main target is to perform a full reconfiguration of the PV array such that *IMI* is minimized. In this study, the proposed GSA technology is applied to the objective function (*IMI*) to obtain an optimal full reconfiguration of the PV modules for any PS PV array. The number of the design variables of the optimized problem is based on the size of the PV array. The GSA code is built using MATLAB environment [21]. The overall performance ratio (*PR*) of the PV array is tested for the optimal reconfigurable array to validate its effectiveness. *PR* is defined by the following formula [10]:

$$PR = \frac{P_{A\,max} \times G_n}{G_{av} \times P_{dc}} \quad (6)$$

where $P_{A\,max}$ is the array's maximum output power, G_{av} is the average solar irradiation of the PV array, and P_{dc} is the rated dc output power of the PV array.

4 GSA

The GSA is a meta-heuristic physics-based optimization technique. The GSA depends mainly on the laws of gravity and motion. In this algorithm, agents (masses) are objects which attract each other by the gravity force resulting in a global movement of all objects towards heavier masses objects. This concept is based on the gravity law, where the gravity force between any two particles is directly proportional to the product of the two masses. This means that the heaviest mass that contributes to the high gravitational force is an optimum solution within the search space [13]. There are four specifications for each mass: position, inertial mass, active gravitational mass, and passive gravitational mass. The mass position is a candidate solution and the gravitational and inertial masses are determined using a fitness function. For a system consists of N masses, the position of the ith mass can be written as follows:

$$X_i = \left(x_i^1, \ldots., x_i^d, \ldots. x_i^n\right) \qquad \text{for } i = 1, 2, ..., N \quad (7)$$

where n is the dimension of the problem, and x_i^d is the position of the ith mass in the dth dimension. Generally, the masses are initially generated randomly in the search space. At any time t, the gravitational force acting on mass i from mass j is defined as follows [14]:

$$F_{ij}^{d}(t) = G(t)\frac{M_{pi}(t)\times M_{aj}(t)}{R_{ij}(t)+\varepsilon}\left(x_j^d(t) - x_i^d(t)\right) \quad (8)$$

where M_{pi} is the passive gravitational mass of the mass i, M_{aj} is the active gravitational mass of the mass j, $G(t)$ is the gravitational constant at a time t, ε is a small constant, and $R_{ij}(t)$ is the Euclidian distance between the two masses i and j, and it can be expressed as follows:

$$R_{ij}(t) = \left\|x_i(t), x_j(t)\right\|_2 \quad (9)$$

It is supposed that the total force that acts on the mass i in the dth dimension be a random weighted sum of dth components of the forces exerted from the other masses.

$$F_i^d(t) = \sum_{j=1, j\neq i}^{N} rand_j \, F_{ij}^d(t) \quad (10)$$

where $rand_j$ is a random number varying from 0 to 1.

Based on the law of motion, the acceleration of the mass i at a time t and in a direction dth is written as follows:

$$a_i^d(t) = \frac{F_i^d(t)}{M_{ii}(t)} \quad (11)$$

where M_{ii} is the inertial mass of the ith mass.

Moreover, the velocity and position of the mass i in the dth dimension are updated by using the following formulas, respectively:

$$v_i^d(t+1) = rand_i \times v_i^d(t) + a_i^d(t) \quad (12)$$

$$x_i^d(t+1) = x_i^d(t) + v_i^d(t+1) \quad (13)$$

where $rand_i$ is a random number varying from 0 to 1 to give a randomized feature to the search.

At starting, $G(t)$ is initialized with an initial value G_o and then decreases with time to control the search accuracy. In the proposed algorithm, $G(t)$ is described by the following equation:

$$G(t) = G_o \, e^{-\alpha(t/T)} \quad (14)$$

where α is a constant, t is the current iteration, and T is the maximum number of iterations.

The gravitational and inertial masses are calculated by using the fitness function. It is assumed that these masses are equal and can be updated by the following formulas:

$$M_{ai} = M_{pi} = M_{ii} = M_i \quad \text{for } i = 1, 2, ..., N \quad (15)$$

$$m_i(t) = \frac{fit_i(t) - worst(t)}{best(t) - worst(t)} \quad (16)$$

$$M_i(t) = \frac{m_i(t)}{\sum_{j=1}^{N} m_j(t)} \quad (17)$$

where $fit_i(t)$ is the fitness value of the mass i at time t, and best(t) and worst(t) are defined to a minimization problem as follows:

$$best(t) = \min_{j\in\{1,...,N\}} fit_j(t) \quad (18)$$

$$worst(t) = \max_{j\in\{1,...,N\}} fit_j(t) \quad (19)$$

Moreover, the last two equations are reversed for a maximization problem. The complete flowchart of the GSA approach is shown in Fig. 2.

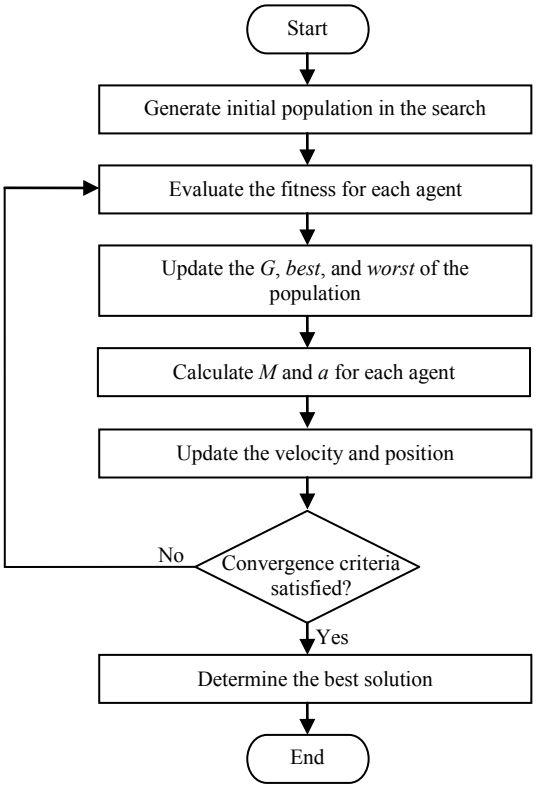

Fig. 2. Flowchart of the GSA approach.

5 Simulation Results and Discussion

In this study, the chosen configuration of a PV array is 6 x 4. Two different PV modules are used to test the GSA-based reconfigurable PV array. The practical PV modules are Shell PowerMax Ultra SQ85-P solar module and Kyocera multicrystal KC200GT. The typical electrical characteristics of these PV modules under standard test conditions (STC) (module temperature 25 ºC, AM 1.5 spectrum, irradiance 1000 W/m^2) are listed in Table I [22], [23]. The iterative method presented in [20] is used to determine the unknown parameters of the single diode PV model. Table II shows the complete parameters of the PV model for two different PV modules. In this study, the GSA technology is applied to minimize the objective function (*IMI*) for obtaining an optimal full reconfiguration of the PV modules for any PS PV array. The problem is an integer optimization problem and the number of design variables of the optimized problem is 24. These design variables are the irradiance level of the PV modules. The solar irradiation under normal conditions is 1000 W/m^2 and the irradiation under PS conditions is 500 W/m^2. Therefore, the optimal value of design variable may be equal 1000 or 500 W/m^2. There is a limitation with the number of PS PV modules in the optimized problem, which varies from PS scenario to another. Based on the GSA approach described in Section 4, the parameters that affect the performance of the GSA are G_o, α, and T. These parameters control the search accuracy and expedite the convergence process. In this study, the optimal chosen GSA characteristics are illustrated in Table III.

Modelling of the PV array under study is carried out using MATLAB/SIMULINK environment. To verify the proposed GSA-based reconfigurable PV array, a detailed comparison should be made with other PV array configurations. The simulation results are performed using an Intel(R) Core(TM) i7-3630QM CPU @ 2.4GHz Processor, 8 GB RAM, 64-bit operating system, PC. The time required to execute the optimization process is included in the comparisons. Different

scenarios are investigated in the following subsections to check the proposed reconfigurable PV array under different partial shading and PV modules conditions.

TABLE I
TYPICAL ELECTRICAL CHARACTERISTICS OF PV MODULES UNDER THE STC

	SQ85-P	KC200GT
I_{sc}	5.45 A	8.21 A
V_{oc}	22.2 V	32.9 V
I_{mp}	4.95 A	7.61 A
V_{mp}	17.2 V	26.3 V
P_{max}	85 W	200 W
K_V	-0.0645 V/ºC	-0.123 V/ºC
K_I	0.0014 A/ ºC	0.00318 A/ ºC
N_s	36	54

TABLE II
PARAMETERS OF THE PV MODEL UNDER THE STC

	SQ85-P	KC200GT
I_{PV}	5.45 A	8.214 A
I_o	$2.418.\ 10^{-5}$ A	$9.825.\ 10^{-8}$ A
R_s	0.187 Ω	0.221 Ω
R_p	360.12 Ω	415.405 Ω
a	1.31	1.3

TABLE III
GSA CHARACTERISTICS

G_o	100
α	20
T	100

Scenario (1):

This scenario presents a single row PS condition. The PV modules are Shell PowerMax Ultra SQ85-P solar modules. Fig. 3(a) and (b) indicates the irradiance levels of the PV array with TCT configuration and GSA-based full reconfigurable PV array, respectively. Fig. 3(c) points out the fitness function convergence using the GSA. It is worth of noting here that the GSA has the merit of high speed convergence. The power versus voltage (*P-V*) curves of the PV array are shown in Fig. 3(d). It can be noted that the generated power of the GSA-based reconfigurable PV array is greater than that of the TCT configuration by 9% and also is smoother than it. Moreover, a detailed comparison is made among the TCT configuration, the MIQP-based full reconfigurable PV array, and GSA-based full reconfigurable PV array, as shown in Table IV to check the PV array performance. It is important to realize that the generated power and PR of the GSA-based reconfigurable PV array is slightly higher than that of the conventional MIQP-based array due to the high accuracy of the PV model. In additions, the time of the optimization process of the GSA technology is deeply slower than that of the MIQP technology. This leads to a fast operation of the PV array under PS conditions when it is applied as well as a contribution to the reduction of PS losses is achieved.

Scenario (2):

The double row PS condition is considered in this scenario. Shell PowerMax Ultra SQ85-P solar modules are used. Fig. 4(a) and (b) indicates the irradiance levels of the PV array with TCT configuration and GSA-based full reconfigurable

1000	1000	1000	1000
1000	1000	1000	1000
1000	1000	1000	1000
1000	1000	1000	1000
1000	1000	1000	1000
500	500	500	500

(a)

500	1000	1000	1000
1000	1000	1000	500
1000	1000	1000	1000
1000	1000	1000	500
1000	1000	1000	1000
1000	1000	500	1000

(b)

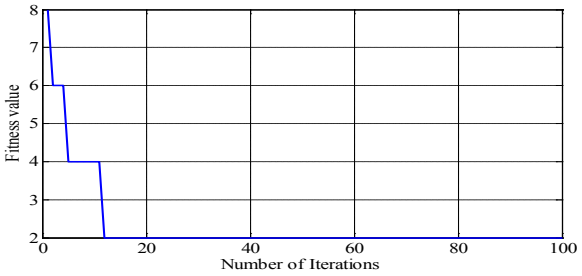

(c)

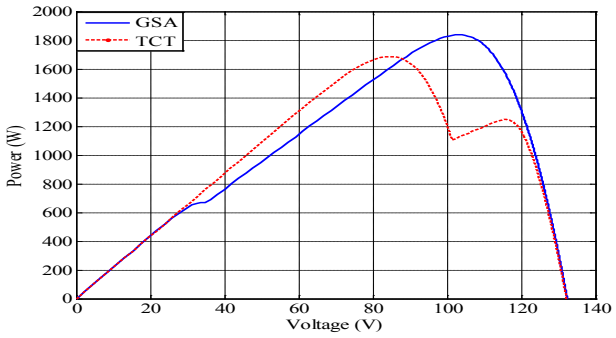

(d)

Fig. 3. Results of Scenario (1). (a) Irradiance levels of the PV array with TCT. (b) Irradiance levels of the GSA-based full reconfigurable array. (c) Fitness function convergence. (d) *P-V* curves.

TABLE IV
COMPARISON OF PV ARRAY CONFIGURATION FOR SCENARIO (1)

	Modules' powers at $P_{A\,max}$ (W)				$P_{A\,max}$ (W)	PR	IMI	Power change w.r.t. TCT (%)	Time (s)
TCT	85.0	85.0	85.0	85.0	1687	0.92	20	.....	.....
	85.0	85.0	85.0	85.0					
	85.0	85.0	85.0	85.0					
	85.0	85.0	85.0	85.0					
	85.0	85.0	85.0	85.0					
	-3.2	-3.2	-3.2	-3.2					
MIQP [10]	84.9	84.9	84.9	**41.8**	1834	0.98	2	+8.7	18.5
	81.1	81.1	81.1	81.1					
	81.1	81.1	81.1	81.1					
	84.9	84.9	**41.8**	84.9					
	84.9	**41.8**	84.9	84.9					
	41.8	84.9	84.9	84.9					
GSA	**42.2**	84.8	84.8	84.8	1838.5	0.983	2	+9	0.31
	84.8	84.8	84.8	**42.2**					
	81.4	81.4	81.4	81.4					
	84.8	84.8	84.8	**42.2**					
	81.4	81.4	81.4	81.4					
	84.8	84.8	**42.2**	84.8					

PV array, respectively. Fig. 4(c) points out the fitness function convergence using the GSA. The *P-V* characteristics of the PV array are illustrated in Fig. 4(d). It can be noted that the generated power of the GSA-based reconfigurable PV

array is greater than that of the TCT configuration by 23.1%. The *P-V* curve with the proposed technology is smoother than that of TCT configuration. This helps in the reduction of MPPT misleading. Moreover, Table V lists a comparison among the GSA-based full reconfigurable PV array and other PV configurations. It can be realized that the generated power and PR of the GSA-based reconfigurable PV array is slightly higher than that of the MIQP-based array. Therefore, the proposed algorithm contributes to the reduction of PS losses. In additions, the optimization time of the GSA technology is very short. The high performance of the proposed reconfigurable PV array reflects the GSA merits and proper design of the GSA model.

Scenario (3):

In this scenario, a quarter array PS condition is applied. For an extensive verification of the proposed algorithm, another type of PV modules (KC200GT) is used. Fig. 5(a) and (b) indicates the irradiance levels of the PV array with TCT configuration and GSA-based full reconfigurable PV array, respectively. The *P-V* curves of the PV array are illustrated in Fig. 5(c). Table VI shows a comparison between the proposed GSA-based full reconfigurable PV array and TCT configurable array. It can be noted that the generated power increases by 9.13% using the proposed reconfigurable array than that of the TCT configurable array. Furthermore, with the GSA-based array, *PR* rises to unity and *IMI* falls to zero. This provides with a good perspective for the PS losses reduction.

TABLE V

COMPARISON OF PV ARRAY CONFIGURATION FOR SCENARIO (2)

	Modules' powers at $P_{A\,max}$ (W)				$P_{A\,max}$ (W)	PR	IMI	Power change w.r.t. TCT (%)	Time (s)
TCT	85.0	85.0	85.0	85.0	1333.8	0.78	32	.....	.....
	85.0	85.0	85.0	85.0					
	85.0	85.0	85.0	85.0					
	85.0	85.0	85.0	85.0					
	-3.2	-3.2	-3.2	-3.2					
	-3.2	-3.2	-3.2	-3.2					
MIQP [10]	80.8	80.8	**41.2**	80.8	1630	0.96	2	+21.8	21.7
	80.8	**41.2**	80.8	80.8					
	83.1	**40.6**	83.1	**40.6**					
	41.2	80.8	80.8	80.8					
	40.6	83.1	**40.6**	83.1					
	80.8	**41.2**	80.8	80.8					
GSA	**40.0**	82.2	82.2	82.2	1642.5	0.97	2	+23.1	0.35
	82.2	**40.0**	82.2	82.2					
	82.2	82.2	82.2	**40.0**					
	41.2	82.6	**41.2**	82.6					
	41.2	82.6	82.6	**41.2**					
	82.2	82.2	**40.0**	82.2					

1000	1000	1000	1000
1000	1000	1000	1000
1000	1000	1000	1000
500	500	1000	1000
500	500	1000	1000
500	500	1000	1000

(a)

500	1000	1000	1000
1000	1000	1000	500
1000	500	1000	1000
1000	1000	1000	500
500	1000	1000	1000
1000	1000	500	1000

(b)

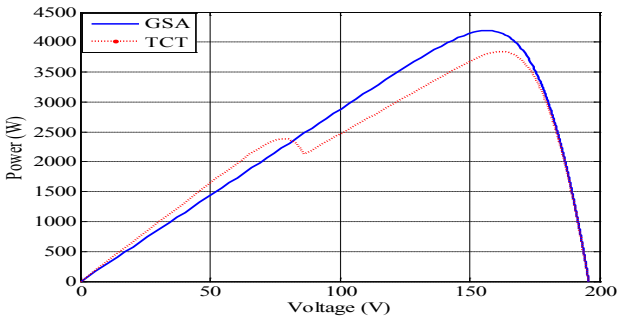

(c)

Fig. 5. Results of Scenario (3). (a) Irradiance levels of the PV array with TCT. (b) Irradiance levels of the GSA-based full reconfigurable array. (c) *P-V* curves.

TABLE VI

COMPARISON OF PV ARRAY CONFIGURATION FOR SCENARIO (3)

	Modules' powers at $P_{A\,max}$ (W)				$P_{A\,max}$ (W)	PR	IMI	Power change w.r.t. TCT (%)	Time (s)
TCT	172.9	172.9	172.9	172.9	3842	0.91	9	.....	.....
	172.9	172.9	172.9	172.9					
	172.9	172.9	172.9	172.9					
	97.8	97.8	196.7	196.7					
	97.8	97.8	196.7	196.7					
	97.8	97.8	196.7	196.7					
GSA	**98.7**	200.0	200.0	200.0	4193	1	0	+9.13	0.33
	200.0	200.0	200.0	**98.7**					
	200.0	**98.7**	200.0	200.0					
	200.0	200.0	200.0	**98.7**					
	98.7	200.0	200.0	200.0					
	200.0	200.0	**98.7**	200.0					

1000	1000	1000	1000
1000	1000	1000	1000
1000	1000	1000	1000
1000	1000	1000	1000
500	500	500	500
500	500	500	500

(a)

500	1000	1000	1000
1000	500	1000	1000
1000	1000	1000	500
500	1000	500	1000
500	1000	1000	500
1000	1000	500	1000

(b)

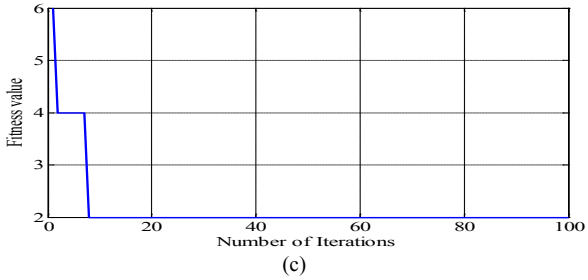

(c)

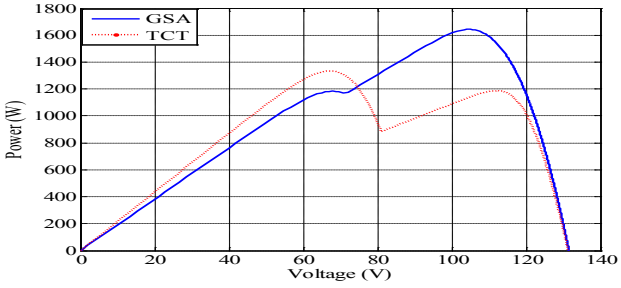

(d)

Fig. 4. Results of Scenario (2). (a) Irradiance levels of the PV array with TCT. (b) Irradiance levels of the GSA-based full reconfigurable array. (c) Fitness function convergence. (d) *P-V* curves.

6 Conclusion

This paper has introduced a novel application of the GSA technology to optimally full reconfigure the PV array for the PS losses reduction. The target of the optimized problem is to minimize the irradiance level mismatch index, which is the sum of squares of the differences between the total irradiance levels of the PV rows. The GSA was applied successfully to solve the optimized problem producing an optimal reconfigurable PV array. Several comparisons were made to verify the validity of the GSA-based reconfigurable PV array. It can be claimed from the results the following points:

1) The generated power and the performance ratio of the GSA-based reconfigurable PV array is greater than that of TCT configurations and is close to that of MIQP-based reconfigurable PV array. Moreover, the optimization time of the GSA technology is rigorously slower than that of MIQP technology, providing high suitability for real time applications.
2) The simulation results of the GSA-based reconfigurable PV array are better than that of the mentioned configurations under different PS and PV modules conditions.
3) The high performance of the proposed reconfigurable PV array reflects the GSA merits and proper design of the GSA model.

Therefore, with the application of the GSA technology, an optimal reconfigurable PV array can be achieved and PS losses can be reduced.

References

[1] PV Power Plants 2014 Industry Guide, online: http://www.pvresources.com.

[2] Hany M. Hasanien, "Shuffled frog leaping algorithm for photovoltaic model identification", *IEEE Transactions on Sustainable Energy,* vol. 6, no. 2, pp. 509-515, April 2015.

[3] M. Drif, P. J. Perez, J. Aguilera, and J. D. Aguilar, "A new estimation method of irradiance on a partially shaded PV generator in grid-connected photovoltaic system," *Renewable Energy*, vol. 33, no. 9, pp. 2048–2056, Feb. 2008.

[4] H. Patel and V. Agarwal, "MATLAB-based modeling to study the effects of partial shading on PV array characteristics," *IEEE Transactions on Energy Conversion*, vol. 23, no. 1, pp. 302–310, March 2008.

[5] A. Maki and S. Valkealahti, "Power losses in long string and parallel-connected short strings of series-connected silicon-based photovoltaic modules due to partial shading conditions," *IEEE Transactions on Energy Conversion*, vol. 27, no. 1, pp. 173–183, March 2012.

[6] K. Ishaque and Z. Salam, "A deterministic particle swarm optimization maximum power point tracker for photovoltaic system under partial shading condition," *IEEE Transactions on Industrial Electronics*, vol. 60, no. 8, pp. 3195–3206, August 2013.

[7] E. I. Batzelis, I. A. Routsolias, and S. A. Papathanassiou, "An explicit PV string model based on the Lambert W function and simplified MPP expressions for operation under partial shading," *IEEE Transactions on Sustainable Energy*, vol. 5, no. 1, pp. 301–312, January 2014.

[8] S. Moballegh and J. Jiang, "Modeling, prediction, and experimental validations of power peaks of PV arrays under partial shading conditions," *IEEE Transactions on Sustainable Energy*, vol. 5, no. 1, pp. 293–300, January 2014.

[9] A. Bidram, A. Davoudi, and R. S. Balog, "Control and circuit techniques to mitigate partial shading effects in photovoltaic arrays," *IEEE Journal of Photovoltaics*, vol. 2, no. 4, pp. 532–546, October 2012.

[10] M. Z. Shams El-Dein, M. Kazerani, and M. M. A. Salama, "Optimal photovoltaic array reconfiguration to reduce partial shading losses," *IEEE Transactions on Sustainable Energy*, vol. 4, no. 1, pp. 145–153, January 2013.

[11] D. Nguyen and B. Lehman, "An adaptive solar photovoltaic array using model-based reconfiguration algorithm," *IEEE Transactions on Industrial Electronics*, vol. 55, no. 7, pp. 2644–2654, July 2008.

[12] G. Velasco, F. Guinjoan, R. Pique, M. Roman, and A. Conesa, "Electrical PV array reconfiguration strategy for energy extraction improvement in grid-connected PV systems," *IEEE Transactions on Industrial Electronics*, vol. 56, no. 11, pp. 4319–4331, November 2009.

[13] E. Rashedi, H. Nezamabadi-pour, and S. Saryazdi, "GSA: A gravitational search algorithm," *Information Sciences*, vol. 179, pp. 2232-2248, 2009.

[14] S. Duman, Y. Sonmez, U. Guvenc, and N. Yorukeren, "Optimal reactive power dispatch using a gravitational search algorithm," *IET Generation, Transmission and Distribution*, vol. 6, no. 6, pp. 563-576, 2012.

[15] T. Niknam, M. R. Narimani, R. Azizipanah-Abarghooee, and B. Bahmani-Firouzi, "Multiobjective optimal reactive power dispatch and voltage control: A new opposition-based self-adaptive modified gravitational search algorithm," *IEEE Systems Journal,* vol. 7, no. 4, pp. 742-753, December 2013.

[16] A. Bhattacharya, and P. K. Roy, "Solution of multi-objective optimal power flow using gravitational search algorithm," *IET Generation, Transmission and Distribution*, vol. 6, no. 8, pp. 751-763, 2012.

[17] W. S. Tan, M. Y. Hassan, H. Abdul Rahman, M. P. Abdullah, and F. Hussin, "Multi-distributed generation planning using hybrid particle swarm optimization-gravitational search algorithm including voltage rise issue," *IET Generation, Transmission and Distribution*, vol. 7, no. 9, pp. 929-942, 2013.

[18] L. D. Coelho, V. C. Mariani, N. Tutkun, and P. Alotto, "Magnetizer design based on a quasi-oppositional gravitational search algorithm," *IEEE Transactions on Magnetics,* vol. 50, no. 2, 7017404, February 2014.

[19] Y. A. Mahmoud, W. Xiao, and H. H. Zeineldin, "A parameterization approach for enhancing PV model accuracy," *IEEE Transactions on Industrial Electronics*, vol. 60, no. 12, pp. 5708–5716, December 2013.

[20] M. G. Villalva, J. R. Gazoli, and E. R. Filho, "Comprehensive approach to modeling and simulation of photovoltaic arrays," *IEEE Transactions on Power Electronics*, vol. 24, no. 5, pp. 1198–1208, May 2009.

[21] Release 2013 a, "MATLAB," The Math Works press, February 2013.

[22] Shell PowerMax Ultra SQ85-P solar module Datasheet. Shell Solar Industries LLP. CA, USA. [online]. Available: http://www.shell.com/solar

[23] KC200GT High Efficiency Multicrystalline Photovoltaic Module Datasheet. Kyocera. [online]. Available: http://www.kyocera.com.sg/products/solar/pdf/kc200gt.pdf